PPPL-3239 - Preprint: March 1997, UC-420, 427

Calculations of alpha particle loss for reversed magnetic shear in the Tokamak Fusion Test Reactor

M. H. Redi, R. B. White, S. H. Batha, F. M. Levinton, D. C. McCune
Plasma Physics Laboratory, Princeton University, P. O. Box 451
Princeton, New Jersey 08540

ABSTRACT

Hamiltonian coordinate, guiding center code calculations of the toroidal field ripple loss of alpha particles from a reversed shear plasma predict both total alpha losses and ripple diffusion losses to be greater than those from a comparable non-reversed magnetic shear plasma in the Tokamak Fusion Test Reactor (TFTR) [Fusion Technol. **21**, 1324 (1992)]. High central q is found to increase alpha ripple losses as well as first orbit losses of alphas in the reversed shear simulations. A simple ripple loss model, benchmarked against the guiding center code, is found to work satisfactorily in transport analysis modelling of reversed and monotonic shear scenarios. Alpha ripple transport on TFTR affects ions within r/a = 0.5, not at the plasma edge. The entire plasma is above threshold for stochastic ripple loss of alpha particles at birth energy in the reversed shear case simulated, so that all trapped 3.5 MeV alphas are lost stochastically or through prompt losses. The 40% alpha particle loss predictions for TFTR suggest that reduction of toroidal field ripple will be a critical issue in the design of a reversed shear fusion reactor.

PACS numbers 52.55.Pi, 52.65.Cc, 52.65.-y, 52.55.Fa

DISCLAIMER

Portions of this document may be illegible in electronic image products. Images are produced from the best available original document.

I. INTRODUCTION

In the recently discovered enhanced reversed magnetic shear mode[1] of tokamak operation, remarkably reduced transport of thermal ion energy and particles has been found at all the major world tokamaks[2-5]. Reversed magnetic shear represents a major modification of the usual q profiles, with a high central q value and non-monotonic q(r) achieved by deliberate modification of plasma startup conditions. Each point in a toroidal plasma magnetic equilibrium can be characterized by the parameter $q = d\Phi/d\Psi$, the rate of change of the toroidal flux with poloidal flux; magnetic shear, $s = (r/q)dq/dr$, is the dimensionless radial derivative of this plasma safety factor, q. In the Tokamak Fusion Test Reactor (TFTR) the enhanced reversed shear mode, with reduced thermal ion transport, arises in reversed magnetic shear plasmas when the neutral beam heating power is above a threshold, about 20 MW.

Retention of fast ions in tokamak fusion reactors will be essential for utilizing alpha particle and other fast ion heating. Toroidal field (TF) ripple can drive high levels of fast particle stochastic ripple loss, particularly in regions of high plasma q and q'. Consequently there has been concern that high central q in reversed shear may cause unacceptable losses of fast ions. High ripple loss rates in reversed shear have been found in recent measurements of triton burnup on JT-60U for 1 MeV tritons[6] and in predictive simulations of 3.5 MeV alpha particles in ITER scenarios[7-10]. This paper presents calculations of alpha particle orbit loss and, in particular, of stochastic ripple loss for an enhanced reversed shear, deuterium-tritium experimental scenario on TFTR.

A new, fast, Hamiltonian coordinate, guiding center code has been used for these simulations of the reversed shear experiment. The guiding center code simulations are compared to those previously published[11] for experiments on TFTR with a monotonic shear profile, at both high and low current and neutral beam heating power. Simulation parameters are presented in Section II and the guiding center code results are discusssed in Section III. In Section IV the results are compared to those found with a simple model of stochastic ripple loss presently used in transport analysis. A summary and conclusion are presented in Section V.

II. GUIDING CENTER CODE SIMULATIONS OF TFTR EXPERIMENTS

Guiding center code simulations which follow the motion of an ensemble of fast particles in toroidal magnetic coordinates over an energy slowing down time are a highly accurate, but relatively time consuming method for the analysis of fast particle loss from tokamak experiments[7-14]. The ORBIT[15] guiding center code has been used to assess the loss rate of fast alpha particles due to TF ripple in TFTR experiments[11,14] and in several ITER designs[7-10]. A new fast version of this code[9] making use of a rapid, accurate algorithm for the stochastic free domain is applied here to the loss of alpha particles from a TFTR enhanced reversed shear plasma. Guiding center code simulations were

carried out for complete orbit calculations as well as with the fast algorithm for the stochastic loss domain, and with accelerated collisional effects.

The ORBIT guiding center code simulations follow an ensemble of 256 to 10,000 alpha particles, initially at 3.5 MeV, in a realistic toroidal magnetic geometry for one alpha particle slowing down time, incorporating the collisional effects of pitch angle scattering and energy slowing down as well as TF ripple and first orbit loss. In Table I and in Figure 1 are found comparisons of the plasma parameters for three TFTR experimental scenarios. The geometry and collision rates utilized in the simulations correspond to these scenarios, which were deuterium only. The alpha particle inital radial profiles correspond to the alpha birth profile in similar deuterium-tritium experiments, as measured by neutron collimator on TFTR.

The Table shows that the reversed shear and the high current, monotonic shear cases are plasmas with similar minor and major radii, toroidal field, final levels of neutral beam power, plasma current and edge q. The monotonic shear cases with large major radius at high and low current were studied in Ref. 11. Figure 1 shows the constant plasma current and neutral beam power which produce a monotonic q profile in the high current case (Figs. 1b, 1d, 1f). The reversed shear case has a prolonged phase of low beam power heating during the current ramp, followed by a high beam power heating phase at full current (Figs. 1a, 1c, 1e). The two scenarios have very different q profiles (Figs. 1e, 1f). In Fig. 1f, the q profile is monotonic with q(0) less than 1.0, changing little during the duration of the pulse. On the other hand, the q profile of the reversed shear plasma evolves in response to the changing plasma current and neutral beam heating conditions. The entire profile q(r) decreases and qmin shifts inward as the beam power increases. At the end of the beam pulse, the plasma has high central and edge safety factors (q(0)~3, q(a)~7), with the minimum q occuring at about one-third the minor radius.

Simulations of the reversed shear experiment were carried out to study the behavior of alpha particles near the end of the neutral beam heating phase. The parameters in Table I for reversed shear correspond to this time, 3.0 sec. This paper will focus on comparison of the high current monotonic shear and reversed shear plasmas. The guiding center code simulations utilized a magnetic geometry obtained with the PEST16 code using q and pressure profiles from a TRANSP17 analysis for the experiment. Simulations for several alpha profiles were carried out, all of which are consistent with Abel inverted neutron profile measurements of TFTR DT experiments. Most simulations were carried out with an alpha profile described by (1-(r/a)2)5. Steeper radial profiles, (1-(r/a)2)7 and (1-(r/a)2)9 were also studied.

To investigate the role of collisions in alpha particle ripple transport, the collision frequencies for both pitch angle scattering and energy slowing down were estimated following the standard formulations[18]. These depend on the electron density, the electron temperature and the level of plasma impurities. In Ref. 11 collisional ripple loss was found to be increased by long slowing down times and by high pitch angle scattering rates. The energy slowing down time is shorter and the pitch angle collision frequency is higher for the enhanced reversed shear plasma than for the monotonic shear

cases primarily because of higher electron density in the reversed shear experiment as a result of the reduced outward particle diffusion. The relative effects of the shorter slowing down time and the higher pitch angle scattering frequency roughly cancel, so that the orbit effects of toroidal field ripple and plasma current will determine differences in alpha particle losses between the reversed and monotonic shear experiments. Figure 2 shows the radial behavior of the energy slowing down rate and the perpendicular energy diffusion rate along with the constant, approximate collision frequencies used in simulations of the reversed shear plasma. The electron densities, temperatures and impurity concentrations were taken from experimental measurements of TFTR shot 84011. During one alpha energy slowing down time of 0.08 sec, an alpha particle with unity pitch (v///v) at the magnetic axis performs 56,000 toroidal transits in the reversed shear case. Most of the guiding center code simulations were carried out with 256 alpha particles.

III. SIMULATION RESULTS AND DISCUSSION

In Tables II through V are shown the simulation results for the TFTR scenarios considered. Tables III and IV reproduce some ORBIT simulation results of the TFTR monotonic shear experiments from Ref. 11, for comparison to the reverse shear alpha loss simulations. The simulations of the reversed shear case in Table II were carried out for an alpha particle density profile of the form $n_a(r)=(1-(r/a)^2)^5$ and with either radially varying or spatially constant collision rates. Because of the steep density and temperature profiles observed in enhanced reversed shear plasmas, simulations were carried out incorporating radial dependence of the energy slowing down and pitch angle scattering collision rates (Fig. 2). Note that the perpendicular energy diffusion rate is twice the pitch angle scattering rate. The constant collision rates used (pitch angle collision frequency, nPA=0.065 sec-1; alpha slowing down time, te = 0.08 sec) are seen to be weighted toward the center of the plasma. Most of the guiding center code results were obtained with constant collision rates, since use of radially varying collision rates made no difference in the alpha particle energy and particle loss fractions.

To investigate the role of collisions in alpha loss, simulations were carried out with and without collisional effects and with and without toroidal field ripple orbit effects. Very different alpha loss patterns are revealed by the simulations of reversed and montonic shear. Tables II and III survey both collisional and ripple transport effects and show that the reversed shear case is predicted to lose 40% of the fusion alpha particles over one slowing down time, while in the monotonic shear case with comparable edge q, only 23% of the alpha particles are lost. Table II also shows that much of the 40% total losses in the reversed shear case arises from the 18% first orbit losses. These appear in the table for calculations without either ripple transport or collisions. The combined effects of the large banana width of alpha particles on TFTR (proportional to q) and a high central q increase the first orbit losses in reversed shear compared to monotonic shear by a factor of 3.

The collisionless stochastic ripple loss for reversed shear is predicted to be 15%, while for the comparable monotonic shear case, collisionless ripple loss is 6%. For both reversed and monotonic

shear the role of collisional lost orbit enhancement alone, if toroidal field ripple is absent, is small (< 2% increased particle loss). Simulations of the monotonic q case show[11] that collisions are unimportant unless combined with ripple transport and that a synergy between these effects increases non-first orbit losses by a factor of 2.4. A characteristic "synergy" parameter is defined as the non-first orbit alpha losses found with both collisions and ripple divided by the sum of the non-first orbit alpha loss found with ripple only and with collisions only. A similar synergy for the effect of collisions enhancing alpha ripple losses on TFTR is not found for reversed shear, for which S = 1.3. Lower synergy results because of a very high first orbit loss fraction and because high average plasma q drives large collisionless ripple losses.

The guiding center code simulations of reversed shear show that including collisions and ripple leads to an increase in total alpha losses to about twice the first orbit loss level. We will show in the next section that the entire plasma is above the threshold for alpha particle ripple loss in the reversed shear plasma. About one-third of the alphas are born trapped and are quickly lost, either from prompt losses or collisionless stochastic ripple diffusion.

In Figure 3 is shown the time dependence of the alpha loss fraction from the reversed shear and high current monotonic shear simulations which included both collisions and ripple. The high first orbit loss and collisionless stochastic ripple loss in reversed shear bring the early loss fraction to 33%, followed by a few percent of collisional scattering dependent losses. The $t^{1/2}$ diffusive signature of collisional stochastic ripple transport is apparent in the monotonic shear case but is masked by high first orbit and collisionless stochastic ripple processes in reversed shear. Many of the differences between the reversed shear and high current monotonic shear plasmas, including the reduced ripple/ collisional synergism, are due to the fact that in reversed shear, first orbit losses are high, greatly reducing the trapped particle fraction after the first bounce period. It is interesting to compare this case to the low current, monotonic shear large major radius TFTR case (Table IV) which also exhibits high first orbit losses. Predictions of total alpha particle loss from reversed magnetic shear at high beam power and plasma current are as high as predicted for the low current and low beam power experiment. Reversed magnetic shear, while characterized by very high confinement of thermal ions, is seen to lack the good alpha particle confinement usually associated with high plasma current.

The 0.9 MA monotonic shear case had edge magnetic q of 14 and consequently a much stronger ripple diffusion than the reversed shear plasma. This low current plasma had high first orbit losses, like the reversed shear case and also low synergism, S=1.4, in the alpha loss simulations. The stronger synergistic effect of collisions and ripple in simulations of high current TFTR monotonic shear plasmas suggested that reduced impurity levels could be effective in keeping alpha ripple losses minimal. However, because of the already low Zeff (2.2), low edge q and reduced synergy in the reversed shear simulations, we expect that reducing impurity levels would not significantly reduce alpha losses for these plasmas.

Table V shows the effect of the flat and radially varying collision rates on the alpha particle losses, along with the effect of accelerating the pitch angle scattering and energy slowing down colli-

sions by factors of 10 and 100. The collisionally accelerated cases made use of the fast stochastic threshold algorithm9. Most simulations were carried out for 256 particles. For 256 particles and a 40% loss rate, the Monte Carlo error is ~ +/- 4%, while for 10,000 particles, the 38% loss rate has an error of ~ +/- 0.6%. Within the statistical error, the use of radially varying collision rates is not found to change the fraction of lost particles.

Table V also shows the loss fractions obtained for different alpha particle radial profiles, using constant collision rates. First orbit losses drop slightly as the profile is steepened, but the collisionless stochastic ripple loss increases sightly at the same time, maintaining the sum of very rapid particle loss from the plasma at about 40%. The total loss does not change within the error of the simulations when the peakedness of the alpha profile is increased. All three profiles simulated are consistent within error bars, with the neutron collimator data and thus the alpha particle birth profile in reversed shear deuterium-tritium plasmas. Variation in the alpha profile steepness does not have a strong effect on the loss rate, in part because of the banana width broadening after a few transits as seen in Figure 4.

The guiding center code has also been used to study the effect of ripple transport on the alpha particle profile for these TFTR cases. It was of interest to see if ripple loss from the alpha profile is concentrated near the plasma edge since TF ripple increases exponentially with radius. For reversed shear, since ripple transport depends strongly on plasma q and q', there has been speculation that the alpha profile might be ripple broadened to the minimum q radius. Ten thousand particles were used for these Monte Carlo simulations to improve statistics for the profile comparisons.

Several alpha profiles obtained during the evolution of each scenario are shown in Figure 4. In the enhanced reversed shear case the initial alpha profile is much more peaked than in monotonic shear, because of the dramatically improved core transport of thermal ions. After 8 toroidal transits 16% first orbit loss has occurred in the reversed shear scenario but only 4% loss has occurred in the monotonic shear case. The profiles after 8 toroidal transits show banana width broadening for both scenarios and higher (25%) central alpha losses in the reversed shear case. After one slowing down time the alpha profiles show a similar shape in both scenarios, with most alpha losses occuring within r/a = 0.5. Ripple-broadening to q_{min} is not seen in reversed shear. It is also clear that alpha ripple loss is not greatest at the plasma edge for TFTR, even in monotonic shear experiments. This is likely due to the relatively large alpha particle ion banana width. We have found that simulations of alphas in ITER-like scenarios, with smaller banana width, do show higher relative loss near the plasma edge for cases of high TF ripple.

New measurements of reversed shear alpha profiles with the pellet charge exchange (PCX) diagnostic[19] reveal a hollow alpha density profile in the center of the TFTR for very deeply trapped alphas (pitch = -0.05) at E = 1.71 MeV, but with the alpha distribution measured at 0.53 MeV being peaked at the magnetic axis20. The difference between these observations and our simulations is likely to be resolved by noting that the present guiding center code simulations survey the behavior of a distribution of alphas isotropic in pitch angle after one slowing down time, while the PCX observations sample a narrow pitch angle spectrum of deeply trapped alphas, the alpha particles known to be most

affected by TF ripple orbit loss. Work is in progress to further clarify the PCX observations and to analyze lost alpha data for these plasmas.

IV. STOCHASTIC RIPPLE LOSS THRESHOLD MODELS

A. POLOIDALLY DEPENDENT STOCHASTIC THRESHOLD ALGORITHM

The collisionally accelerated simulations in Table V made use of a new poloidally dependent algorithm for the alpha particle stochastic ripple diffusion threshold, δ_{WGRB}[9]. Following early work by Goldston, White and Boozer[21], if the toroidal field ripple, defined as

$$dT_F = (B_{MAX}-B_{MIN}) / (B_{MAX}+B_{MIN})$$

is greater than the threshold $dWGR_B$ at the ion bouncepoint, the ion is subject to stochastic ripple diffusion and will be rapidly lost from the plasma. To improve rapid stochastic ripple loss modelling, White has included the effect of poloidal and energy dependence in this stochastic loss criterion though an analytic calculation for a threshold, which includes toroidal precession of fast ions.

Figure 5 shows the confined domains for the reversed shear and high current monotonic shear scenarios using the new threshold algorithm, as a function of alpha particle energy. Confinement, with bounded periodic bounce tip motion and no stochastic ripple loss, is predicted for trapped alpha particles whose bounce points lie in the shaded regions shown in the figure. At the alpha particle birth energy of 3.5 MeV, the stochastic diffusion loss region occupies the whole plasma in the TFTR reversed shear plasma equilibrium. All trapped particles are quickly lost through first orbit or stochastic ripple diffusion. Passing alpha particles slow down and are pitch angle scattered into trapped orbits, for which there are confinement regions at lower energies. At high energies the confinement domains cover less of the plasma cross section in reversed shear than in the monotonic shear comparison case. As an ion slows down the shaded confinement domain increases so that at thermal velocities no stochastic ripple loss is predicted and neoclassical and anomalous losses predominate.

B. GOLDSTON WHITE BOOZER STOCHASTIC THRESHOLD CRITERION

A stochastic threshold-based model has been installed in the TRANSP analysis code[17] to calculate ripple loss of fast ions in TFTR DT experiments[2]. This model is based on the simple Goldston, White and Boozer criterion[21] (GWB) in which the toroidal field ripple is compared to a threshold proportional to

$$\delta_{GWB} = (e/Npq)^{3/2}(1/\rho q').$$

Here N is the number of toroidal field coils, ρ is the ion gyro radius, ε is the inverse aspect ratio a/R and q' the plasma shear, $q' = r\, dq/dr$. In this model if the ripple, δ_{TF}, is greater than the threshold δ_{GWB} at the ion bouncepoint, the ion is subject to stochastic ripple diffusion and is deleted from the analysis code calculations. The criterion specifies a confinement domain, roughly describing a circle about the magnetic axis. It does not include any poloidal nor all the energy dependence contained in the more accurate stochastic free domain algorithm[9] used for Figure 5. The loss regions of the more accurate

threshold δ_{WGRB} at the highest energies are clearly not circles centered on the magnetic axis.

A renormalization of the simple TRANSP GWB model was obtained by benchmarking the model[14] with ORBIT calculations of standard TFTR cases. This has been useful for analyses of TFTR L mode and supershot cases. The renormalized threshold is $\delta_S = (1/A)\delta_{GWB}$ with A = 2, and corresponds to a lower stochastic threshold for alpha particles on TFTR which is 1/2 the GWB threshold. Figure 6 shows the alpha particle ripple diffusion energy losses calculated by TRANSP with this model for the reversed shear case. A, on the abscissa, is the ratio of the GWB stochastic threshold to the applied TRANSP stochastic threshold. The alpha ripple energy losses calculated by TRANSP for several cases, varying A, are compared to the guiding center code losses calculated with ripple and collisions. A=1 corresponds to the unrenormalized GWB threshold. For the enhanced reversed shear case, the guiding center code losses of 40% are roughly equal to those with the standard benchmarked TRANSP model at A=2. A similar TRANSP/ORBIT comparison carried out for ITER, with strong up/down ripple asymmetry, showed that the TFTR renormalization had to be reduced by an order of magnitude[8]. Since there is no threshold for alpha ripple loss in reversed shear, the details of the more accurate threshold algorithm are not critical to calculating the particle losses. For neutral beam ions with initial energies near 100 keV, the details of the more accurate, poloidally dependent threshold criterion are likely to be of more importance, since for these ions a threshold to stochastic ripple diffusion does exist.

V. CONCLUSION

Simulations with a Hamiltonian coordinate guiding center code of a reversed magnetic shear plasma in TFTR predict that alpha particle losses are near 40%, about double the total alpha losses from a comparable plasma with a monotonic shear profile. In the reversed shear case, the entire plasma is above threshold for stochastic loss of alpha particles at birth energy. All trapped alphas are lost at birth through stochastic ripple loss or first orbit losses, as $q(r) > 2$ throughout the plasma. Pitch angle scattering of passing particles refills the trapped distribution and leads to continued alpha loss throughout the slowing down process.

It is found that the simple renormalized Goldston, White, Boozer ripple loss model used in the TRANSP code for TFTR leads to alpha ripple losses in agreement with the guiding center code simulations for both reversed and monotonic shear cases. The simulations show that transport due to TF ripple, for both monotonic and reversed shear q profiles, lies primarily within r/a = 0.5. Ripple loss is not greatest at the plasma edge, nor is there enhanced ripple broadening of the alpha profile toward minimum q in the reversed shear region. Including radially varying collision rates or increased alpha profile peakedness does not significantly change the predicted losses. Strong synergism between collisions and ripple transport, predicted for high current, monotonic shear plasmas, is not found for reversed shear.

The discovery of enhanced reversed shear plasma configurations with dramatically improved transport holds promise for the future applications of controlled fusion. Yet the 40% losses predicted for fusion alpha particles from a TFTR enhanced reversed shear equilibrium suggests new constraints on the allowed toroidal field ripple for such reactor configurations. Up to 20% simulated losses have already been found for some reversed shear equilibria on ITER[7-10]. The exploitation of reversed shear equilibria for reactor design will require minimal toroidal field ripple and impurity levels to reduce collisional ripple loss and to optimize alpha particle confinement and heating.

ACKNOWLEDGEMENTS

We are glad to thank R. V. Budny for preparing the TRANSP baseline simulations of the reversed shear experiment, J. Manickam for help in obtaining the reversed shear equilibrium, and S. von Goeler for providing data and analysis of a reversed shear deuterium-tritium neutron emission profile. We are also glad to acknowledge discussions with M. C. Zarnstorff, S. M. Medley, M. J. Bell, D. Darrow, M. Petrov, E. Ruskov and S. J. Zweben. This research was supported by U. S. Department of Energy Contract No. DE-AC02-76-CH03073.

REFERENCES

[1] F. M. Levinton, M. C. Zarnstorff, S. H. Batha, M. Bell, R. E. Bell, R. V. Budny, C. Bush, Z. Chang, E. Fredrickson, A. Janos, J. Manickam, A. Ramsey, A. A. Sabbagh, G. L Schmidt, E. J. Synakowski, G. Taylor, Phys. Rev. Lett. **75**, 4417 (1995).

[2] R. J. Hawrylůk, H. Adler, P. Alling, C. Ancher, H. Anderson, J. L. Anderson, J. W. Anderson, V. Arunasalam, G. Ascione, D. Ashcroft, C. W. Barnes, G. Barnes, S. Batha, G. Bateman, M. Beer, M. G. Bell, R. Bell, M. Bitter, W. Blanchard, N. L. Bretz, C. Brunkhorst, R. Budny, C. E. Bush, R. Camp, M. Caorlin, H. Carnevale, S. Cauffman, Z. Chang, C.Z. Cheng, J. Chrzanowski, J. Collins, G. Coward, M. Cropper, D. S. Darrow, R. Daugert, J. Delooper, W. Dorland, L. Dudek, H. Duong, R. Durst, P. C. Efthimion, D. Ernst, H. Evenson, N. J. Fisch, R. Fisher, R. J. Fonck, E. Fredd, E. Fredrickson, N. Fromm, G-Y. Fu, T. Fujita, H. P. Furth, V. Garzotto, C. Gentile, J. Gilbert, J. Gioia, N. Gorelenkov, B. Grek, L.R. Grisham, G. Hammett, G. R. Hanson, W. Heidbrink, Park, P. Parks, S. F. Paul, G. Pearson, E. Perry, R. Persing, M. Petrov, C. K. Phillips, M. Phillips, S. Pitcher, R. Pysher, A.L. Qualls, S. Raftopoulos, S. Ramakrishnan, A. Ramsey, D. A. Rasmussen, M. H. Redi, G. Renda, G. Rewoldt, D. Roberts, J. Rogers, R. Rossmassler, A. L. Roquemore, E. Ruskov, S. A. Sabbagh, M. Sasao, G. Schilling, J. Schivell, G. L. Schmidt, R. Scillia, S. D. Scott, I. Semenov, T. Senko, S. Sesnic, R. Sissingh, C. H. Skinner, J. Snipes, J. R. Stencel, J. Stevens, T. Stevenson, B. C. Stratton, J. D. Strachan, W. Stodiek, J. Swanson, E. Synakowski, H. Takahashi, W. M. Tang, G. Taylor, J. Terry, M. E. Thompson, W. Tighe, J. R. Timberlake, K. Tobita, H. H. Towner, M. Tuszewski, A. Von Halle, C. Vannoy, M. Viola, S. Von Goeler, D. Voorhees, R.T.

Walters, R. Wester, R. B. White, R. Wieland, J. B. Wilgen, M. D. Williams, J. R. Wilson, J. Winston, K. Wright, K. L. Wong, P. Woskov G. A. Wurden, M. Yamada, S. Yoshikawa, K. M. Young, M. C. Zarnstorff, V. Zavereev, and S. J. Zweben, Phys. Rev. Lett. **72**, 3530 (1994).

[3] E. J. Strait, L. L. Lao, M. E. Mauel, B. W. Rice, T. S. Taylor, K. H. Burrell, M. S. Chu, E. A. Lazarus, T. H. Osborne, S. J. Thompson, A. D. Turnbull, Phys. Rev. Lett. **75**, 4421 (1995).

[4] T. Fujita, S. Ide, H. Kimura, Y. Koide, T. Oikawa, S. Takeji, H. Sirai, T. Ozeki, Y. Kamada, S. Ishida and the JT-60 Team, "Enhanced Core Confinement in JT-60U Reversed Discharges", 16th IAEA Fusion Energy Conference (Montreal, Canada, October 1996) Paper IAEA-CN-64/A1-4, to appear in the proceedings.

[5] C. Gormezano for the JET team, "Optimisation of JET plasmas with current profile control", 16th IAEA Fusion Energy Conference (Montreal, Canada, October 1996) Paper IAEA-CN-64/A5-5, to appear in the proceedings.

[6] K. Tobita, T. Nishitani, H. Harano, K. Tani, M. Isobe, T. Fujita, Y. Kusama, G. A. Wurden, H. Shirai, T. Oikawa, T. Fukuda, K. Hamamatsu, S. Ishida, M. Nemoto, T. Kondoh, A. Morioka, H. Kimura, M. Saigusa, S. Moriyama, O. Dacosta, V. I. Afanassiev and the JT-60 Team, "Transport and Loss of Energtic Ions in JT-60U", 16th IAEA Fusion Energy Conference (Montreal, Canada, October 1996) Paper IAEA-CN-64/A5-6, to appear in the proceedings.

[7] M. H. Redi, R. B. White, R. J. Goldston, "TF Ripple Loss of Alpha Particles from the ITER Interim Design: Simulation and Theory", in Plasma Physics and Controlled Nuclear Fusion Research 1996 (Proc. 23rd E. P. S. Conf. Kiev, Ukraine 1996).

[8] M. H. Redi, R. V. Budny, C. O. Miller, R. B. White, Phys. Plas. **3**, 3037 (1996).

[9] R. B. White, R. J. Goldston, M. H. Redi, R. V. Budny, Phys. Plas. **3**, 3043 (1996).

[10] S. V. Konovalov, ITER Physics Design report, 1996.

[11] M. H. Redi, M. C. Zarnstorff, R. B. White, R. V. Budny, A. C. Janos, D. K. Owens, J. F. Schivell, S. D. Scott and S. J. Zweben, Nuclear Fusion **35**, 1191 (1995).

[12] K. Tobita, Nuclear Fusion **35**, 1585 (1995).

[13] K. Tani, T. Takizuka, M. Azumi, H. Kishimoto, Nucl. Fusion **23**, 657 (1983).

[14] M. H. Redi, R. V. Budny, D. S. Darrow, H. H. Duong, R. K. Fisher, A. C. Janos, J. M. McChesney, D. C. McCune, S. S. Medley, M. P. Petrov, J. F. Schivell, S. D. Scott, R. B. White, M. C. Zarnstorff and S. J. Zweben, Nuclear Fusion **35**, 1509 (1995).

[15] R. B. White and M. S. Chance, Phys. Fluids **27** 2455 (1984).

[16] R. Grimm, J. M. Green, J. L. Johnson, Methods Comput. Phys. **16**, 253 (1976).

[17] R. V. Budny, D.C. McCune, M.H. Redi, J. Schivell, R M. Wieland, Phys. Plas. **3**, 4583 (1996).

[18] D. L. Book, Publ. 177-4405, NRL Plasma Formulary, Washington, D. C. (1990) 64pp.

[19] R. K. Fisher, J. M. McChesney, P. B. Parks, H. H. Duong, S. S. Medley, A. L. Roquemore, D. K. Mansfield, R. V. Budny, M. P. Petrov and R. E. Olson, Phys. Rev. Lett. **75**, 846 (1995).

[20] S. Medley, M. Petrov, PPPL, private communication.

[21] R. J. Goldston, R. B. White and A. H. Boozer, Phys. Rev. Lett. **47**, 647 (1981).

TABLE I. COMPARISON OF PARAMETERS FOR TFTR SCENARIOS SIMULATED

	Reversed Shear	Monotonic Shear	
		high current	low current
I_p (MA)	1.6	1.8	0.9
B_T (T)	4.6	4.8	4.5
R (m)	2.6	2.6	2.6
a (m)	0.94	0.96	0.96
P_{inj} (MW)	25	23	13
q_a	7	6	14

TABLE II. GUIDING CENTER CODE ALPHA PARTICLE ENERGY LOSS FOR REVERSED SHEAR CASE (%)

ripple	collisions	Energy Loss	Particle Loss
Simulations with Radial Variation of Collision Rates			
yes	yes	38	40
Simulations with Flat Collision Rates			
no	no	18	18
no	yes	20	20
yes	no	33	33
yes	yes	38	40

TABLE III. GUIDING CENTER CODE ALPHA PARTICLE ENERGY LOSS FOR HIGH CURRENT, MONOTONIC SHEAR CASE (%)

ripple	collisions	Energy Loss	Particle Loss
no	no	6	6
no	yes	6	6
yes	no	12	12
yes	yes	19	23

TABLE IV. COMPARISON OF GUIDING CENTER CODE ALPHA PARTICLE LOSSES FOR THREE TFTR CASES (%)

	Reversed Shear	Monotonic Shear (1.8 MA)	Monotonic Shear (0.9 MA)
First Orbit	18	6	21
Delayed Particle Loss	22	17	13
Total Particle Loss	40	23	34
Total Energy Loss	38	19	32

TABLE V. ALPHA LOSS FRACTIONS CALCULATED WITH ACCELERATED COLLISIONS FOR REVERSED SHEAR (%)

	Energy Loss	Particle Loss
Simulations with Radial Variation of Collision Rates		
No acceleration	38	40
10x acceleration	41	43
100x acceleration	37	41
Simulations with Flat Collision Rates		
No acceleration	38	40
10x acceleration	40	41
100x acceleration	38	40 +/- 4
100x acceleration with 10,000 particles	35	38 +/- 0.6
Simulations for Different Alpha Profiles and 10x Acceleration		
$(1-x^2)^5$	40	41
$(1-x^2)^7$	38	40
$(1-x^2)^9$	36	38

LIST OF FIGURE CAPTIONS

Figure 1.

a) Time dependence of plasma current for the reversed shear case.
b) Time dependence of plasma current for the high current, monotonic shear case.
c) Time dependence of total neutral beam injection for the reversed shear case.
d) Time dependence of total neutral beeam injection for the high current, montonic shear case.
e) q profile for the reversed shear case at early and late times.
f) q profile for the high current, monotonic shear case.

Figure 2.

a) Radial collision rate for energy slowing down in the reversed shear case.
b) Radial collision rate for perpendicular energy diffusion in the reversed shear case.

Figure 3.

Time dependence of alpha loss over one slowing down time from simulations of the reversed shear and the high current, monotonic shear cases.

Figure 4.

a) Guiding center code initial alpha profile and simulation profiles after 8 toroidal transits and after one slowing down time for the reversed shear case.
b) Guiding center code initial alpha profile and simulation profiles after 8 toroidal transits and after one slowing down time for the high current, monotonic shear case.

Figure 5.

a) Confinement region for alpha particles of energy 3.5 MeV in the reversed shear case.
b) Confinement region for alpha particles of energy 3.5 MeV in the high current, monotonic shear profile case.
c) Confinement region for alpha particles of energy 1.75 MeV in the reversed shear case.
d) Confinement region for alpha particles of energy 1.75 MeV in the high current, monotonic shear profile case.
e) Confinement region for alpha particles of energy 0.35 MeV in the reversed shear case.
f) Confinement region for alpha particles of energy 0.35 MeV in the high current, monotonic shear profile case.

Figure 6.

Alpha particle ripple lost energy calculated by TRANSP as a function of A, the inverse multiplier of the GWB threshold for the reversed shear case. ORBIT alpha particle ripple lost energy also shown.

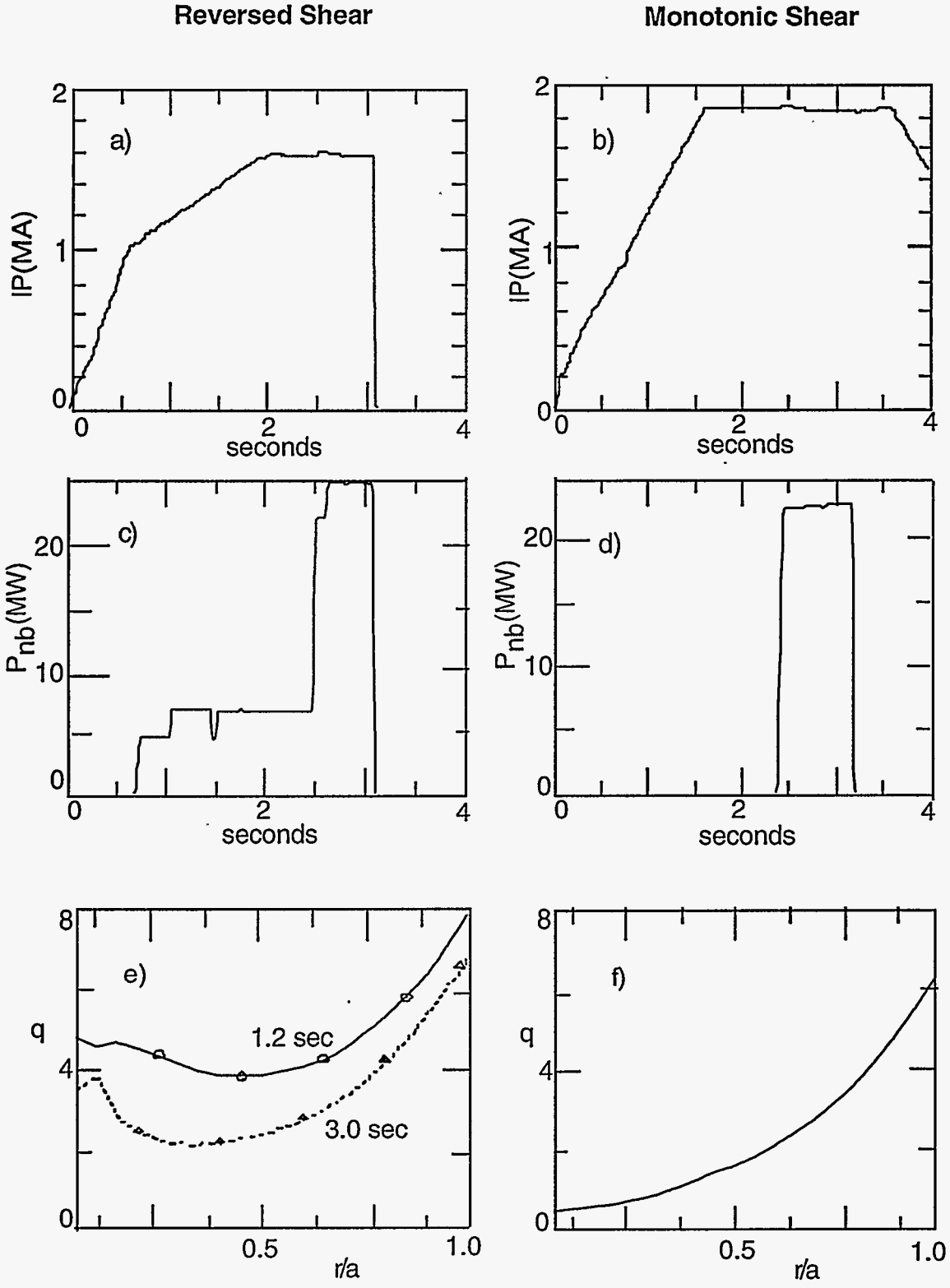
Reversed Shear
Monotonic Shear
a)
b)
IP(MA)
seconds
c)
d)
P_{nb}(MW)
e)
f)
1.2 sec
3.0 sec
q
r/a

Figure 1

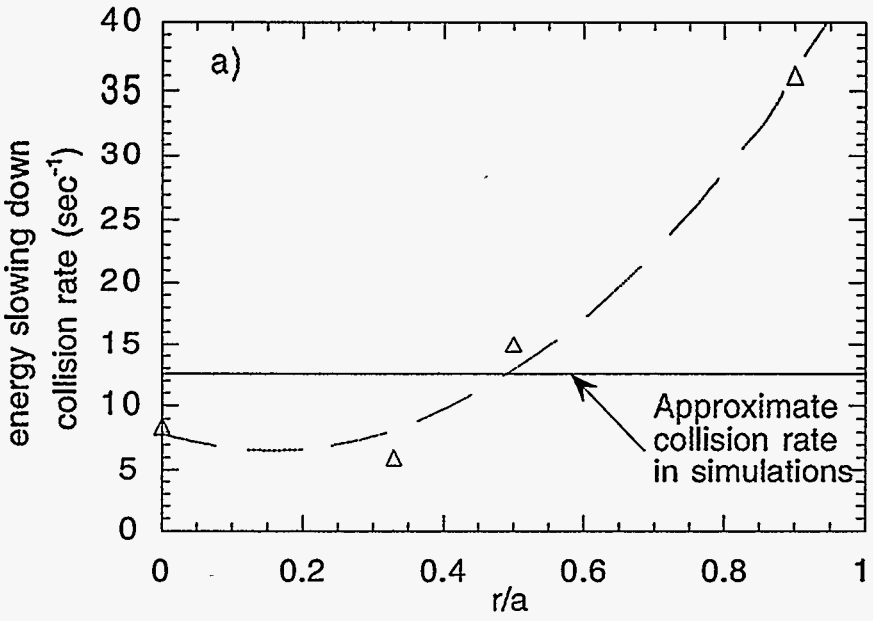
a)
energy slowing down
collision rate (sec^{-1})
40
35
30
25
20
15
10
5
0
0
0.2
0.4
0.6
0.8
1
r/a
Approximate
collision rate
in simulations

Figure 2 a

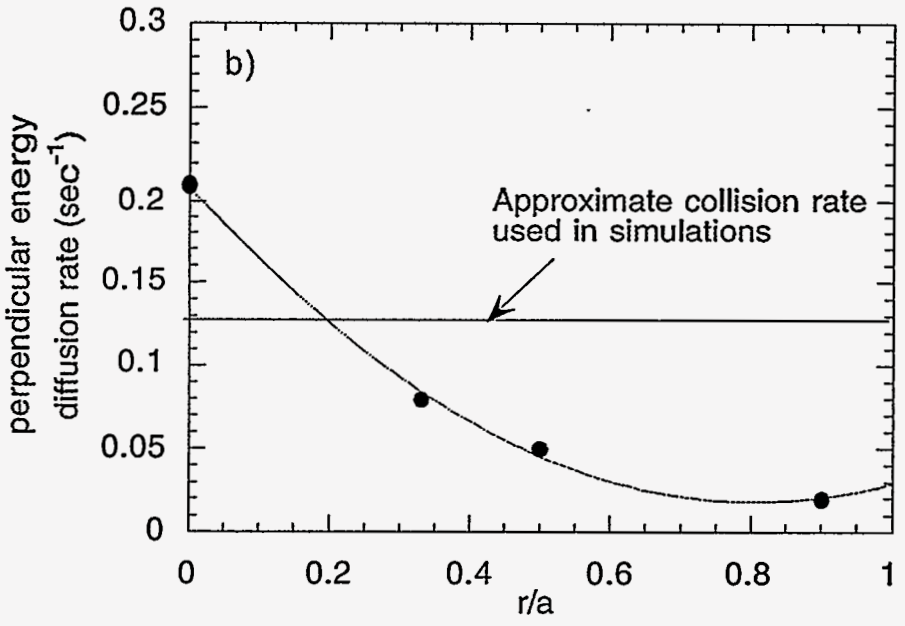
b)
perpendicular energy diffusion rate (sec^{-1})
Approximate collision rate used in simulations
0.3
0.25
0.2
0.15
0.1
0.05
0
0
0.2
0.4
0.6
0.8
1
r/a

Figure 2 b

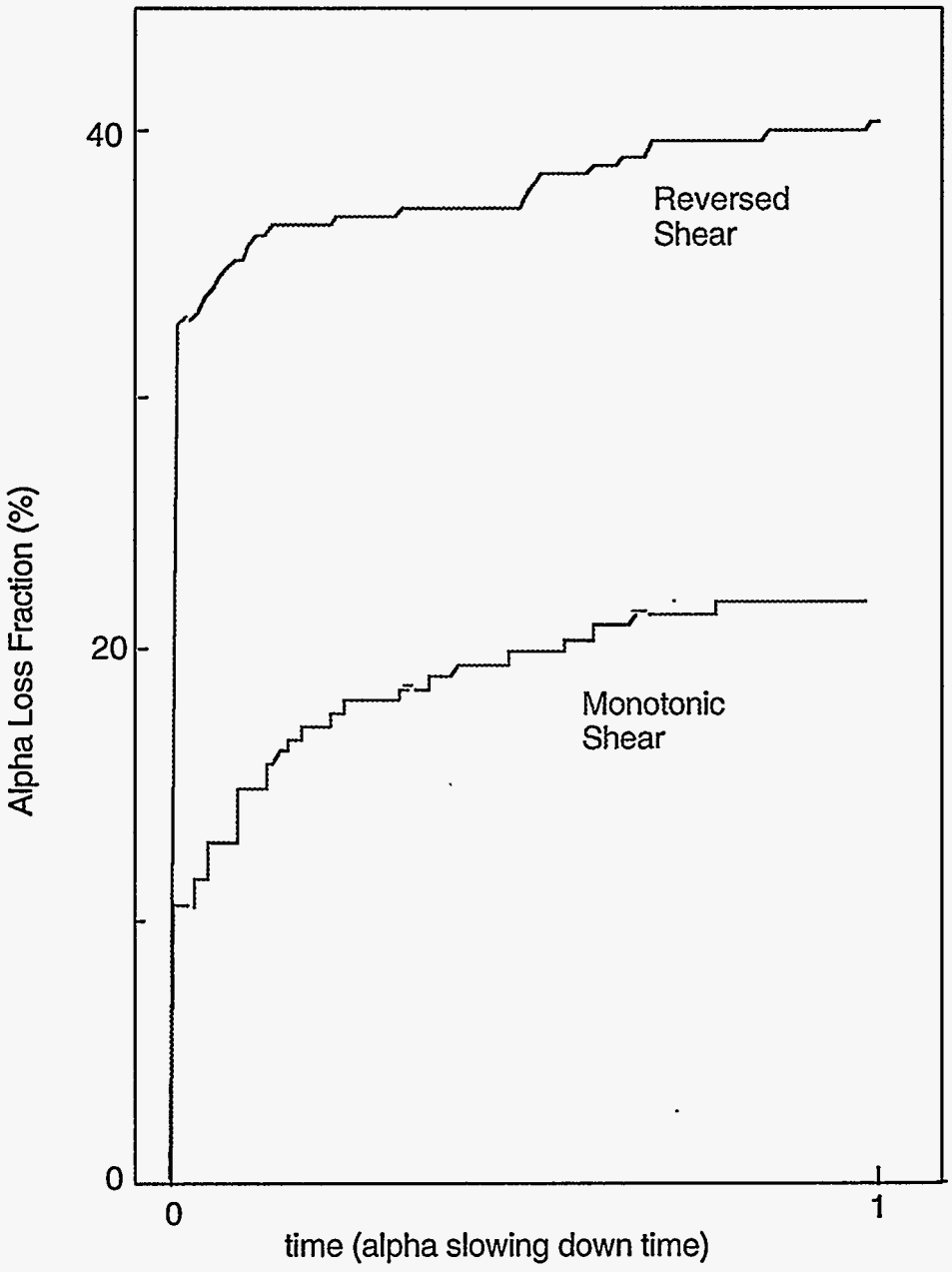
40
20
0
Alpha Loss Fraction (%)
Reversed
Shear
Monotonic
Shear
0
1
time (alpha slowing down time)

Figure 3

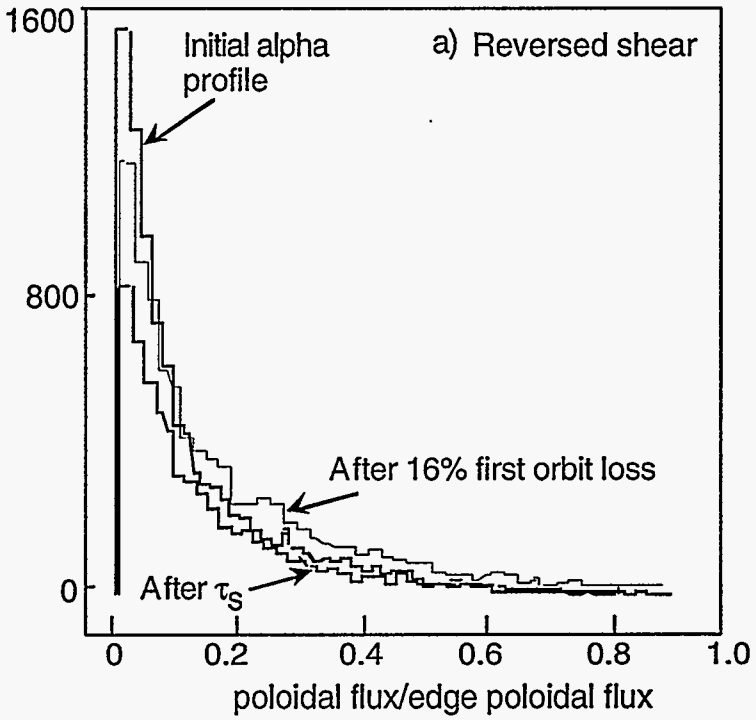
1600
800
0
Initial alpha profile
a) Reversed shear
After 16% first orbit loss
After τ_s
0
0.2
0.4
0.6
0.8
1.0
poloidal flux/edge poloidal flux

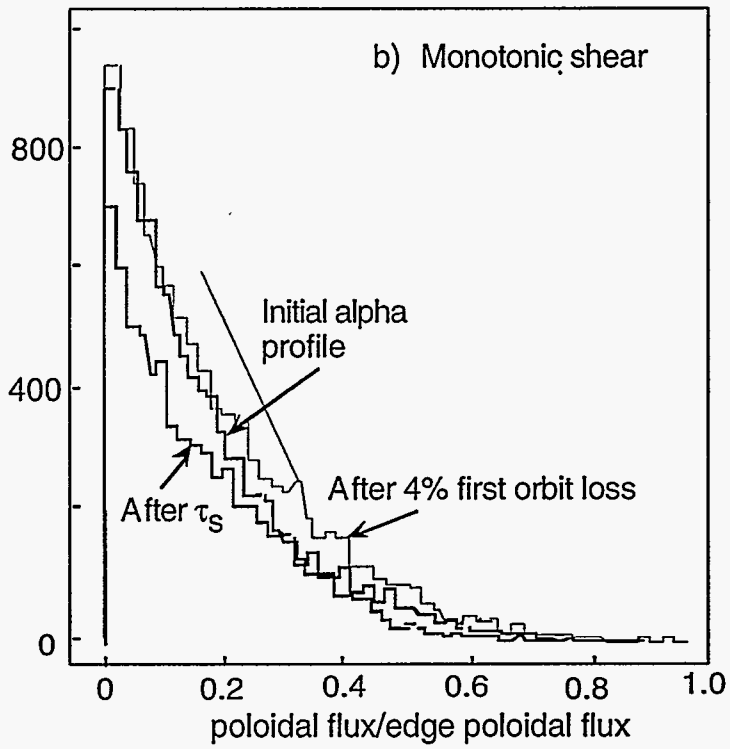
b) Monotonic shear
800
400
0
Initial alpha profile
After 4% first orbit loss
After τ_s
0
0.2
0.4
0.6
0.8
1.0
poloidal flux/edge poloidal flux

Figure 4

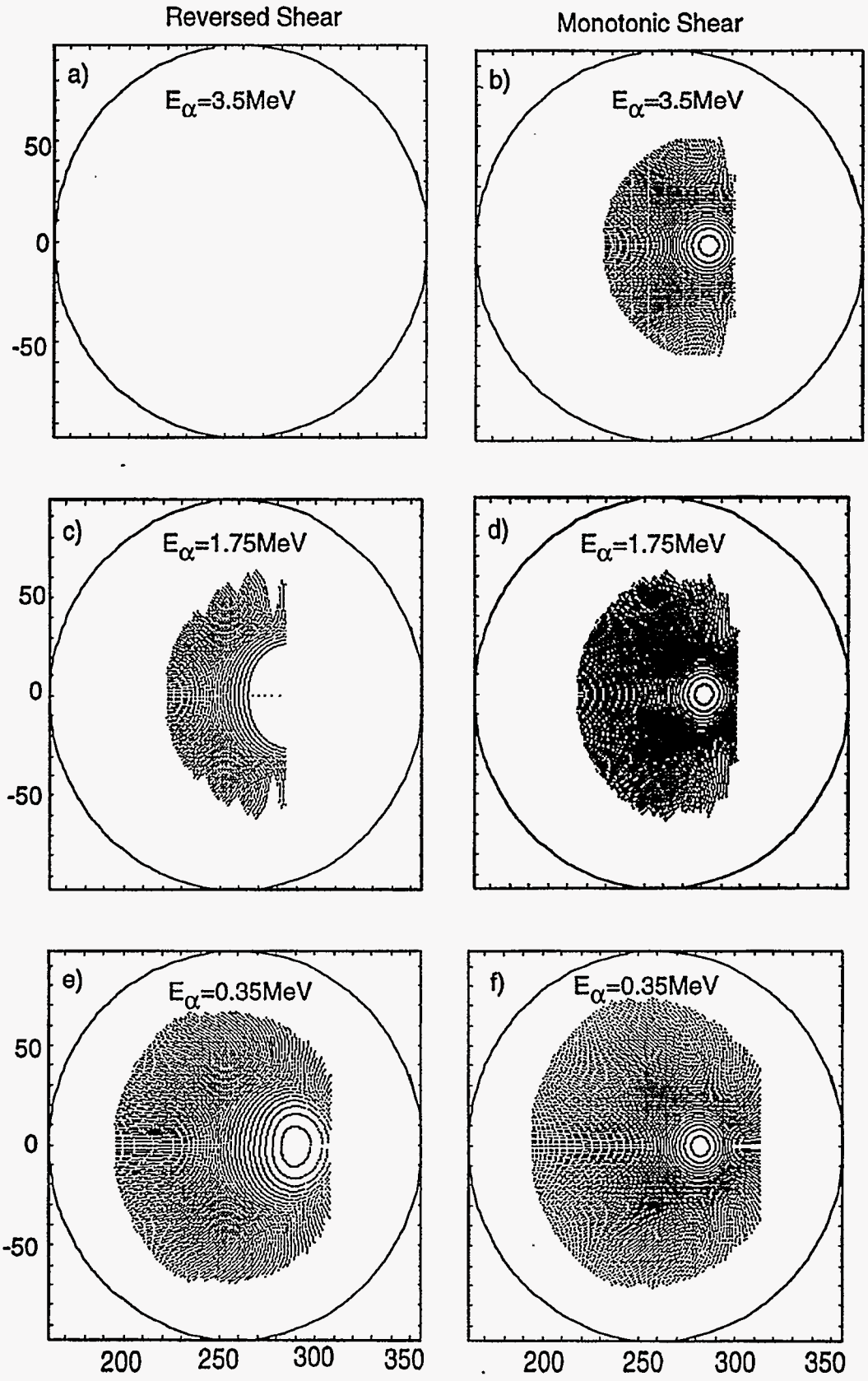
Reversed Shear
Monotonic Shear
a)
E_α=3.5MeV
b)
E_α=3.5MeV
c)
E_α=1.75MeV
d)
E_α=1.75MeV
e)
E_α=0.35MeV
f)
E_α=0.35MeV
50
0
-50
200
250
300
350

Figure 5